

ANALYTIC INCREMENTAL LEARNING FOR SOUND SOURCE LOCALIZATION WITH IMBALANCE RECTIFICATION

Zexia Fan¹, Yu Chen^{1,2}, Qiquan Zhang³, Kainan Chen⁴, Xinyuan Qian^{1*}

¹University of Science and Technology Beijing, Beijing, China

²The Chinese University of Hong Kong, Shenzhen, China

³Tongyi Speech Lab, Alibaba, China

⁴Eigenspace GmbH, Germany

ABSTRACT

Sound source localization (SSL) demonstrates remarkable results in controlled settings but struggles in real-world deployment due to dual imbalance challenges: intra-task imbalance arising from long-tailed direction-of-arrival (DoA) distributions, and inter-task imbalance induced by cross-task skews and overlaps. These often lead to *catastrophic forgetting*, significantly degrading the localization accuracy. To mitigate these issues, we propose a unified framework with two key innovations. Specifically we design a GCC-PHAT-based data augmentation (GDA) method that leverages peak characteristics to alleviate intra-task distribution skews. We also propose an Analytic dynamic imbalance rectifier (ADIR) with task-adaption regularization, which enables analytic updates that adapt to inter-task dynamic. On the SSLR benchmark, our proposal achieves state-of-the-art (SoTA) results of 89.0% accuracy, 5.3° mean absolute error, and 1.6 backward transfer, demonstrating robustness to evolving imbalances without exemplar storage. Code and data will be released.

Index Terms— Sound source localization, Generalized class-incremental learning, Long-tailed distribution, Data augmentation, Adaptive dynamic imbalance rectifier

1. INTRODUCTION

Sound Source Localization (SSL) aims to estimate the DoA of sound sources from multichannel audio. In the context of human-robot interaction, SSL is fundamental for selective auditory attention [1], automatic speech recognition [2], speech enhancement [3, 4, 5], and speaker extraction [6] in multi-speaker and noisy scenarios. Traditional signal processing approaches rely on idealized acoustic assumptions and derive closed-form solutions, such as GCC-PHAT [7], MUSIC [8], and SRP-PHAT [9]. They often perform well under controlled scenarios, but struggle with challenging acoustic conditions such as noisy and strong reverberant environments. Deep learning-based supervised neural SSL has recently demonstrated significant advancements. Existing approaches can be broadly grouped into hybrid [10, 11, 12, 13] and pure neural solutions [14, 15, 16, 17]. The former leverages a deep neural network (DNN) to enhance specific modules of traditional pipelines. While the latter optimizes DNNs to estimate DoA in an end-to-end fashion.

In practice, labeled SSL data is scarce and arrive incrementally, as in robotic audition where DoA annotations evolve over time. A critical problem in this incremental setting is catastrophic forgetting, where the model loses previously acquired knowledge when

This work is supported by National Natural Science Foundation of China (62306029), Beijing Natural Science Foundation (L233032) and Young Elite Scientists Sponsorship Program of the Beijing High Innovation Plan.

*Corresponding author

adapting to new tasks. Class-incremental learning (CIL) has been explored to address this issue, which seeks to integrate new classes while preserving old knowledge. Existing CIL generally spans three paradigms: regularization-based approaches [18, 19] that constrain weight updates to retain information, replay-based approaches [20, 21] that store exemplars for knowledge distillation, and analytic approaches [22, 23, 24, 25] that exploit closed-form solutions for computational efficiency. Building on these foundations, SSL-CIL [26] introduced the first CIL framework for SSL, yet CIL method remain challenged by complex real-world conditions such as repeated class occurrences and class imbalance problems.

These limitations become particularly acute in the generalized CIL (GCIL) setting for SSL, which faces a fundamental challenge: the long-tailed class distributions of DoA data. This manifests in two forms: 1) *Intra-task imbalance* arises within each task, where certain directions dominate training data while minority directions remain severely underrepresented [27, 28]; 2) *Inter-task imbalance* occurs across tasks, with uneven or overlapping class distributions, which induces dynamic biases and exacerbates forgetting [29]. Together, these imbalances make GCIL for SSL particularly difficult, especially when privacy constraints prohibit storing past data.

To tackle these challenges, we propose a novel unified framework, namely SSL-GCIL, that addresses both intra-task and inter-task imbalances. For intra-task imbalance, we introduce a GDA method that exploits GCC-PHAT peak statistics to synthesize samples for tail classes, preserving inter-microphone correlations without requiring external data. For inter-task imbalance, we design ADIR, an analytic classifier whose core adaptive regularization is guided by task-specific statistics (e.g., the Gini coefficient) to effectively mitigate cross-task skews and forgetting [28]. Together, these components form a lightweight, adaptive SSL framework tailored for GCIL. In summary, our contributions are summarized as:

- Our proposal is the first SSL framework that address both intra-task and inter-task imbalances in the GCIL setting, providing an effective solution for long-tailed distributions which alleviate catastrophic forgetting.
- We introduce GDA that exploits GCC-PHAT peak statistics to synthesize tail-class samples, alleviating intra-task imbalance while maintaining statistical consistency and privacy.
- We propose an ADIR, a unified analytic framework that dynamically responds to inter-task class overlaps and distribution skews through its task-adaptive regularization.

We conduct comprehensive experiments on the SSLR benchmark, the experimental results demonstrate the superiority of our proposed SSL-GCIL over SoTA baselines, achieving improvements of 3.2% in accuracy, 1.2° in mean absolute error, and 2.5 in backward transfer.

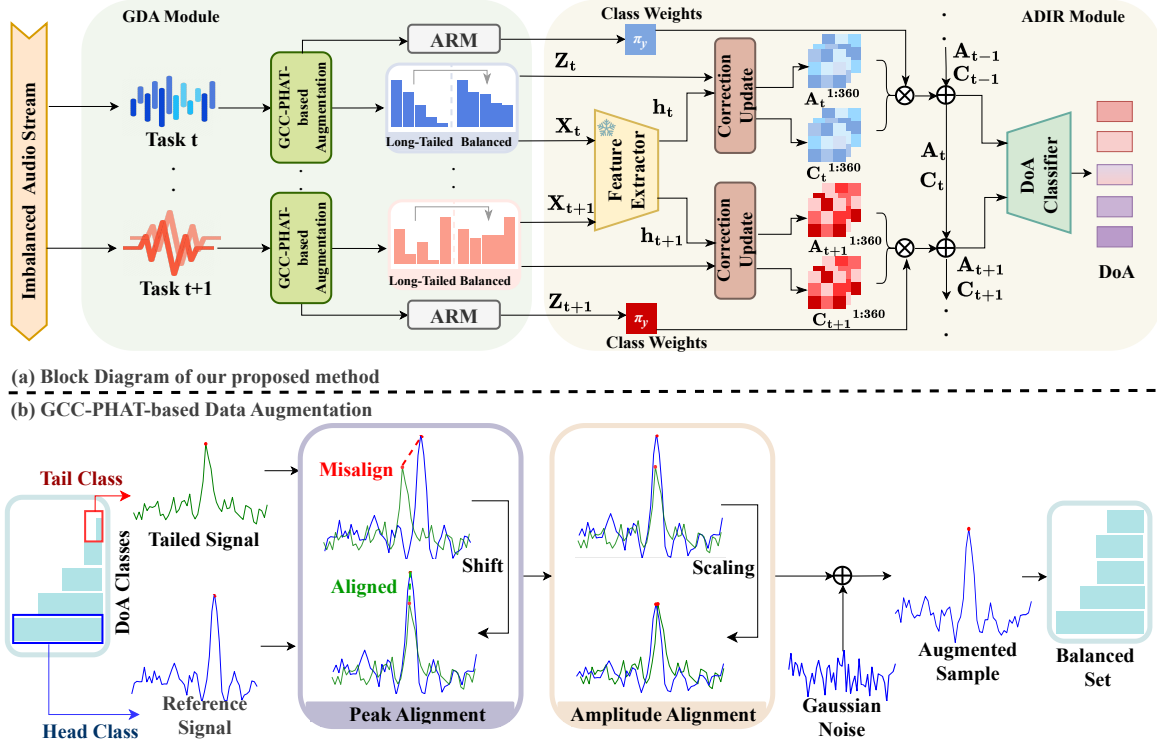


Fig. 1: (a) Block Diagram of our proposed method and (b) GCC-PHAT-based Data Augmentation (\oplus indicates addition).

2. METHOD

In this section, we first formalize the problem of GCIL for SSL and then introduce our proposed method. As illustrated in Fig. 1(a), the framework is composed of two main components: a GDA module for feature enrichment and an ADIR module with a frozen MLP feature extractor to map GCC-PHAT features to DoA probability.

2.1. Problem Formulation

We formulate SSL as a GCIL problem, where data arrives in tasks, each containing new and old sound direction classes with imbalanced distributions. Let $\mathcal{D}_t = \{(\mathbf{x}_i^{(t)}, \mathbf{y}_i^{(t)}, \mathbf{z}_i^{(t)})\}_{i=1}^{N_t}$ denote the training set of task $t \in \{1, \dots, T\}$, where $\mathbf{x}_i^{(t)} \in \mathbb{R}^{P \cdot D_a}$ is the GCC-PHAT feature derived from a P -pair microphone array, D_a being the feature dimension per pair, $\mathbf{y}_i^{(t)} \in \{0, 1\}^{360}$ is the one-hot label indicating the true DoA in $[0^\circ, 360^\circ]$, and $\mathbf{z}_i^{(t)} \in \mathbb{R}^{360}$ is the Gaussian-distributed label generated from $\mathbf{y}_i^{(t)}$ with a peak at the true DoA and standard deviation $\sigma = 5^\circ$. The classes in \mathcal{D}_t follow a long-tailed distribution with up to 60 classes per task. The goal is to train a model $f_\theta : \mathbb{R}^{P \cdot D_a} \rightarrow \mathbb{R}^{360}$ minimizing cumulative loss over tasks without revisiting prior data:

$$\mathcal{L} = \sum_{t=1}^T \mathbb{E}_{(\mathbf{x}, \mathbf{z}) \sim \mathcal{D}_t} [\ell(f_\theta(\mathbf{x}), \mathbf{z})], \quad (1)$$

where ℓ is binary cross-entropy loss, addressing catastrophic forgetting and intra-task imbalance without exemplar storage.

2.2. GCC-PHAT-based Data Augmentation

The GCC-PHAT estimates source directions from inter-microphone time delays. For signals with Fourier transforms $X(f)$ and $Y(f)$, it is defined as

$$R_{xy}(\tau) = \int_{-\infty}^{\infty} \frac{X(f)Y^*(f)}{|X(f)Y^*(f)|} e^{j2\pi f\tau} df, \quad (2)$$

where τ denotes the lag. Empirically, the peaks of GCC-PHAT dominate SSL performance, as they encode critical time-difference cues [15]. To mitigate intra-task imbalance under long-tailed distributions [30], we design a domain-specific augmentation that manipulates these peaks while preserving their statistical structure.

For each task t , the feature vector $\mathbf{x}_i^{(t)} \in \mathbb{R}^{P \cdot D_a}$ is partitioned into P segments (one per microphone pair), each of dimension D_a . Let $N_c^{(t)}$ denote the number of samples in class c at task t . For class c , we compute mean and variance of peak positions $\{p_{c,k}\}$ and amplitudes $\{a_{c,k}\}$ across segments. Let $M_t = \max_c N_c^{(t)}$ be the largest class size and $\alpha = 0.5$ the augmentation rate. For any class with $N_c^{(t)} < \alpha M_t$, we generate $K_c = \lceil \alpha M_t - N_c^{(t)} \rceil$ new samples using Algorithm 1. The procedure shifts and rescales peaks of abundant-class features to match the statistics of tail classes, while injecting low-level noise for diversity. This produces $\tilde{\mathcal{D}}_t$, balancing tail representation without distorting inter-microphone correlations.

2.3. Network Architecture

We adopt a network: a frozen feature extractor followed by a task-adaptive classifier. The input $\mathbf{x} \in \mathbb{R}^{P \cdot D_a}$ is mapped to logits $\hat{\mathbf{z}} \in \mathbb{R}^{360}$ via

$$\mathbf{h} = F_{\text{MLP}}(\mathbf{x}; \mathbf{W}_{\text{MLP}}), \quad \hat{\mathbf{z}} = F_{\text{cls}}(\mathbf{h}; \mathbf{W}_t). \quad (3)$$

where F_{MLP} is a three-layer MLP, with each layer consisting of batch normalization, ReLU and dropout. F_{cls} is a fully-connected layer with dropout. The feature extractor \mathbf{W}_{MLP} is only trained in task 1. For subsequent tasks, \mathbf{W}_{MLP} is frozen and only \mathbf{W}_t is updated.

Algorithm 1 GDA for Tail Class c

Require: Base feature $\mathbf{x}_b \in \mathbb{R}^{P \cdot D_a}$ from abundant class c' , statistics $\{p_{c,k}, a_{c,k}\}_{k=1}^P$

Ensure: Augmented sample \mathbf{x}_{new}

- 1: Initialize $\mathbf{x}_{\text{new}} \leftarrow \mathbf{0}^{P \cdot D_a}$
- 2: **for** segment $k = 1, \dots, P$ **do**
- 3: $\Delta p_k \leftarrow p_{c,k} - p_{c',k}$
- 4: Extract $\mathbf{x}_b^{(k)} \in \mathbb{R}^{D_a}$ from \mathbf{x}_b
- 5: Cyclically shift $\mathbf{x}_b^{(k)}$ by Δp_k
- 6: Scale amplitudes to match $a_{c,k}$
- 7: Add Gaussian noise $\mathcal{N}(0, \sigma_n)$, with $\sigma_n = 0.05 \cdot \max(\mathbf{x}_b^{(k)})$
- 8: Assign segment to \mathbf{x}_{new}
- 9: **end for**
- 10: **return** \mathbf{x}_{new}

2.4. Integration of Analytic Dynamic Imbalance Rectifier

We design the ADIR [28] for the GCIL setting. Unlike conventional CIL where classes across tasks are disjoint, GCIL allows classes to reappear, requiring per-class storage of auto-correlation and cross-correlation matrices. Notably, our framework operates without storing any raw audio data or exemplars, ensuring compliance with privacy constraints in real-world applications.

The detailed procedure is shown in Algorithm 2. For each task t , given the frozen MLP features $\mathbf{H}_t \in \mathbb{R}^{N_t \times 1000}$ and Gaussian-smoothed labels \mathbf{Z}_t , the Adaptive Re-weighting Module (ARM)[28] estimates the optimal weight matrix through

$$\mathbf{W}_t^* = \arg \min_{\mathbf{W}_t} \sum_{c=1}^{360} \pi_c \|\mathbf{Z}_t^{(c)} - \mathbf{H}_t^{(c)} \mathbf{W}_t\|_F^2 + \gamma_t \|\mathbf{W}_t\|_F^2, \quad (4)$$

where $\pi_c = 1/N_c$ is the re-weighting factor for class c , and γ_t is an adaptive regularization parameter to enhance stability. Specifically, $\gamma_t = \gamma_0 \cdot e^{\alpha \cdot (\text{Gini}_t - 0.5)}$, with $\gamma_0 = 100$, $\alpha = 2$, and Gini_t is the Gini coefficient computed as (for $n = 60$ classes):

$$\text{Gini}_t = \frac{\sum_{i=1}^n \sum_{j=1}^n |p_i - p_j|}{2n \sum_{i=1}^n p_i}. \quad (5)$$

the closed-form update is given by

$$\mathbf{W}_t^* = \left(\sum_c \pi_c \mathbf{A}^{(c)} + \gamma_t \mathbf{I} \right)^{-1} \left(\sum_c \pi_c \mathbf{C}^{(c)} \right), \quad (6)$$

with $\mathbf{A}^{(c)} = \mathbf{H}_t^{(c)\top} \mathbf{H}_t^{(c)}$ and $\mathbf{C}^{(c)} = \mathbf{H}_t^{(c)\top} \mathbf{Z}_t^{(c)}$. To handle class reoccurrence in GCIL, $\mathbf{A}^{(c)}$ and $\mathbf{C}^{(c)}$ are maintained per class and updated via recursive least squares.

3. EXPERIMENT

3.1. Dataset

We use the SSLR benchmark [10] where 4-channel audio recordings are sampled at 48 kHz with spatial annotations (all possible microphone pairs are used thus $P=6$). Following the GCIL setting [28], the dataset is partitioned into 10 sequential tasks, denoted as \mathcal{D}_i , where $i = 1, \dots, 10$. Each task comprises up to 60 disjoint DoA classes at 1° resolution. Task 1 introduces 60 new classes, while tasks 2–9 add 30 new classes and 30 previously encountered classes from earlier tasks to mimic persistent sources [30]; task 10 covers the remaining classes.

Algorithm 2 ADIR for GCIL in SSL

Require: Task data $\mathcal{D}_t = \{(\mathbf{x}_i^{(t)}, \mathbf{y}_i^{(t)}, \mathbf{z}_i^{(t)})\}_{i=1}^{N_t}$, frozen feature extractor F_{MLP} , regularization parameters γ_0, α

Ensure: Weight matrix $\mathbf{W}_t^* \in \mathbb{R}^{1000 \times 360}$

- 1: Initialize $\mathbf{A}^{(y)} \leftarrow \mathbf{0}^{1000 \times 1000}$, $\mathbf{C}^{(y)} \leftarrow \mathbf{0}^{1000 \times 360}$, $N(y) \leftarrow 0$ for all classes $y \in \{1, \dots, 360\}$
- 2: **for** each $(\mathbf{x}_i, \mathbf{y}_i, \mathbf{z}_i) \in \mathcal{D}_t$ **do**
- 3: $\mathbf{h}_i \leftarrow F_{\text{MLP}}(\mathbf{x}_i) \in \mathbb{R}^{1000}$ ▷ Extract features
- 4: $y \leftarrow \arg \max(\mathbf{y}_i)$ ▷ Get class index
- 5: $\mathbf{A}^{(y)} \leftarrow \mathbf{A}^{(y)} + \mathbf{h}_i \mathbf{h}_i^\top$ ▷ Update auto-correlation
- 6: $\mathbf{C}^{(y)} \leftarrow \mathbf{C}^{(y)} + \mathbf{h}_i \mathbf{z}_i^\top$ ▷ Update cross-correlation
- 7: $N(y) \leftarrow N(y) + 1$ ▷ Update class count
- 8: **end for**
- 9: Compute $\pi_y \leftarrow 1/N(y)$ for all y with $N(y) > 0$
- 10: Compute Gini_t using Eq. (5)
- 11: Set $\gamma_t \leftarrow \gamma_0 \cdot e^{\alpha \cdot (\text{Gini}_t - 0.5)}$ ▷ Adaptive regularization
- 12: Compute $\mathbf{A}_{1:t} \leftarrow \sum_{y=1}^{360} \pi_y \mathbf{A}^{(y)}$, $\mathbf{C}_{1:t} \leftarrow \sum_{y=1}^{360} \pi_y \mathbf{C}^{(y)}$
- 13: **return** $\mathbf{W}_t^* \leftarrow (\mathbf{A}_{1:t} + \gamma_t \mathbf{I})^{-1} \mathbf{C}_{1:t}$

For input, we extract GCC-PHAT features $\mathbf{x}_i^{(t)} \in \mathbb{R}^{6 \times 51}$ from 170 ms segments, corresponding to 51 delay coefficients per microphone pair. One-hot DoA labels $\mathbf{y}_i^{(t)}$ are used for evaluation, while Gaussian-smoothed targets $\mathbf{z}_i^{(t)}$ ($\sigma = 5^\circ$) are adopted for training. Test sets $\mathcal{D}_t^{\text{test}}$ include only the classes of task t , and evaluation is performed cumulatively on $\mathcal{D}_1^{\text{test}}, \dots, \mathcal{D}_t^{\text{test}}$ to track forgetting.

To simulate realistic long-tailed dynamics, each task follows an exponential decay distribution with task-specific imbalance. Specifically, the decay rate increases from $\lambda_1 = 0.05$ to $\lambda_{10} = 0.5$, with

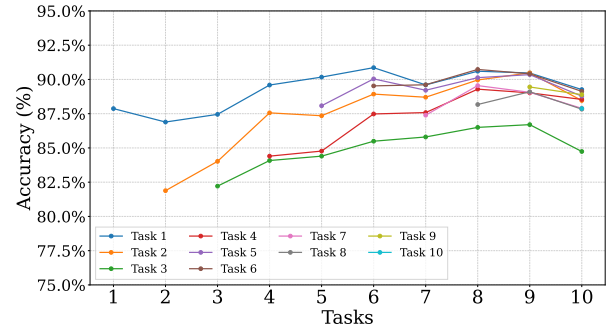
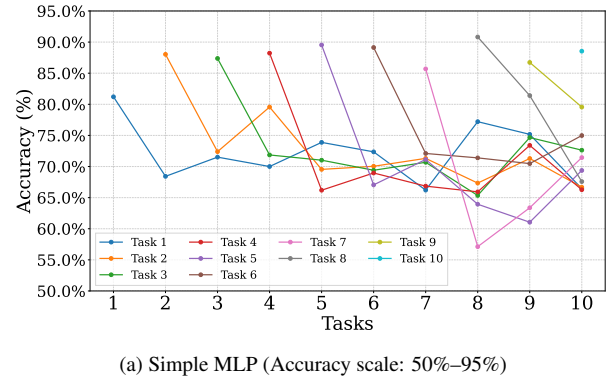


Fig. 2: Comparison of performance curves between the baseline method and our proposed SSL-GCIL approach.

Table 1: Performance comparison of different methods under varying SNR conditions. Models are trained on clean data and tested on noisy data. (‘↑’ indicates that higher scores are preferable while ‘↓’ indicates that lower scores are preferable. * indicates the upper bound.)

SNR	Joint Training*			iCaRL [20]			LwF [18]			ACIL [30]			GACL [24]			Ours		
	MAE↓	ACC↑	BWT↑	MAE↓	ACC↑	BWT↑	MAE↓	ACC↑	BWT↑	MAE↓	ACC↑	BWT↑	MAE↓	ACC↑	BWT↑	MAE↓	ACC↑	BWT↑
Clean	4.3	93.5	—	5.9	85.8	-3.8	6.4	76.7	-12.8	6.5	85.8	-1.7	6.9	78.3	-1.0	5.3	89.0	1.6
20 dB	6.0	88.4	—	7.9	78.6	-6.9	9.2	69.1	-13.7	8.2	81.7	-1.2	9.3	71.5	-1.2	7.3	84.9	1.0
10 dB	13.7	73.2	—	27.5	46.1	-7.5	20.6	61.4	-11.1	15.8	64.4	-1.3	17.8	64.9	-1.4	15.5	69.0	0.9
0 dB	30.8	42.8	—	38.7	33.4	-4.0	42.8	28.4	-5.1	38.4	35.3	-1.4	38.5	33.6	-1.1	36.9	37.9	0.8
-10 dB	47.5	18.6	—	54.9	9.2	-1.5	58.6	6.2	-0.4	50.1	9.9	-0.3	58.9	7.9	-1.4	51.7	16.0	0.6
Avg.	20.5	63.3	—	27.0	50.6	-4.7	27.5	48.4	-8.6	23.8	55.4	-1.2	26.3	51.2	-1.2	23.3	59.4	1.0

Table 2: Ablation studies under clean conditions (GDA: GCC-PHAT-based data augmentation, ADIR: Adaptive dynamic imbalance rectifier).

GDA	ADIR	MAE↓	ACC↑	BWT↑
✗	✗	7.5	72.0	-17.7
✓	✗	7.4	75.0	-15.8
✗	✓	6.1	82.4	1.4
✓	✓	5.3	89.0	1.6

class counts given by $N_c^{(t)} = \lfloor N_{\max} e^{-\lambda_t(c-1)} \rfloor$, $N_{\max} = 500$. This design yields stronger imbalance across tasks, with varying Gini coefficients to capture long-tailed shifts in real-world SSL.

3.2. Evaluation Metrics

We evaluate performance using three metrics: Mean Absolute Error (MAE), Accuracy (ACC), and Backward Transfer (BWT). Specifically, **MAE** measures the average angular error between predicted and true directions of arrival. **ACC** is the proportion of predictions within a 5° tolerance of the true direction following [1]. **BWT** quantifies forgetting in incremental learning: $BWT = \frac{1}{T-1} \sum_{k=1}^{T-1} (A_{T,k} - A_{k,k})$ where $A_{k,k}$ is the ACC on task k immediately after training, and $A_{T,k}$ is the ACC on task k after training all T tasks. Positive and negative BWT indicates knowledge retention and forgetting, respectively.

3.3. Baselines

We compare our method against four SOTA CIL baselines, i.e., **LwF** [18], **iCaRL** [20], **ACIL** [30] and **GACL** [24]. We adapted them to the same SSL-GCIL setting as ours. In addition, we report a *lower bound* using a simple MLP trained only on the initial task without any incremental adaptation [15], and an *upper bound* using joint training on all tasks with access to the full dataset. To ensure fairness, all baselines employ the same MLP feature extractor pretrained on the first task and frozen thereafter. For Task 1, all parameters are optimized with Adam with a learning rate of 0.001, using a binary cross-entropy loss. For subsequent tasks, the feature extractor \mathbf{W}_{MLP} is kept fixed, and only the classifier weights \mathbf{W}_t are updated under the same training protocol.

3.4. Results

Table 1 presents the comprehensive evaluation results across varying SNR conditions. Under clean conditions, our method achieves the best performance with an MAE of 5.3° , ACC of **89.0%**, and positive BWT of **1.6**, thereby indicating effective knowledge retention without catastrophic forgetting. Compared to the strongest baseline ACIL, we achieve 1.2° lower MAE, **3.1%** higher ACC, and

3.3 higher BWT. The joint training upper bound (MAE: 4.3° , ACC: 93.5%) represents the performance ceiling when all data is available simultaneously, while our method approaches this ideal scenario with only incremental access.

As noise levels increase, all methods experience performance degradation, while our approach consistently maintains the relative advantage. For example, at 20dB SNR, we achieve 7.3° MAE and 84.9% ACC, significantly outperforming ACIL by 0.9° and 3.2% respectively. Under severe -10dB conditions, our method achieves the highest ACC (16.0%) among other incremental learning approaches, demonstrates remarkable noise robustness.

The BWT metric reveals our method’s exceptional resistance to catastrophic forgetting. While all baselines show negative BWT, our method maintains positive BWT across all noise levels, with 0.6 even at -10dB SNR. This confirms that our adaptive regularization and augmentation strategy effectively preserves previously learned knowledge in challenging environments.

Fig. 2(a) illustrates the severe catastrophic forgetting problem of the baseline method [15], where the accuracy on previously learned tasks drops significantly as new tasks are introduced. For instance, after training on Task 10, Task 1’s accuracy drops to 66.5%, showing a decline of nearly 15% from its initial performance. In contrast, our method (Fig. 2(b)) maintains stable performance across all tasks, with accuracies consistently above 84% even after incremental training. The ablation studies in Table 2 confirm that both components contribute significantly: ADIR alone improves BWT from -17.7 to 1.4, effectively mitigating negative backward transfer, while adding GDA further boosts ACC from 82.4% to 89.0%. The combination achieves the best balance between accuracy and stability. Overall, our proposed method consistently outperforms all baselines in most scenarios, demonstrating superior robustness to incremental learning challenges and environmental noise.

4. CONCLUSION

In this paper, we present a novel SSL framework under GCIL that integrates GDA with ADIR, thus successfully alleviates class imbalance in long-tailed distributions and mitigates catastrophic forgetting without requiring exemplar storage. Specifically, the GDA module effectively addresses intra-task imbalance by synthesizing tail-class samples through peak statistics manipulation, while the ADIR component mitigates inter-task imbalance via task-adaptive regularization guided by Gini coefficients. On the SSLR benchmark, our model achieves state-of-the-art results, with 89.0% accuracy, a mean absolute error of 5.3° , and a backward transfer of 1.6, consistently outperforming all baselines. For future work, we plan to explore extensions of integrating audio-visual signals for SSL and the online adaptation strategy.

5. REFERENCES

- [1] Y. Chen, X. Qian, Z. Pan, K. Chen, and H. Li, “LocSelect: Target speaker localization with an auditory selective hearing mechanism,” in *Proc. IEEE Int. Conf. Acoust., Speech, Signal Process.*, 2024, pp. 8696–8700.
- [2] X. Zhang, Q. Zhang, H. Liu, T. Xiao, X. Qian, B. Ahmed, E. Ambikairajah, H. Li, and J. Epps, “Mamba in Speech: Towards an alternative to self-attention,” *IEEE/ACM Trans. Audio, Speech, Lang. Process.*, vol. 33, pp. 1933–1948, 2025.
- [3] Q. Zhang, A. Nicolson, M. Wang, K. K. Paliwal, and C. Wang, “DeepMMSE: A deep learning approach to MMSE-based noise power spectral density estimation,” *IEEE/ACM Trans. Audio, Speech, Lang. Process.*, vol. 28, pp. 1404–1415, 2020.
- [4] Q. Zhang, X. Qian, Z. Ni, A. Nicolson, E. Ambikairajah, and H. Li, “A time-frequency attention module for neural speech enhancement,” *IEEE/ACM Trans. Audio, Speech, Lang. Process.*, vol. 31, pp. 462–475, 2023.
- [5] Qiquan Zhang, Hongxu Zhu, Xinyuan Qian, Eliathamby Ambikairajah, and Haizhou Li, “Exploring length generalization for transformer-based speech enhancement,” *IEEE TASLP*, vol. 33, pp. 2690–2704, 2025.
- [6] J. Xu, K. Hu, C. Xu, T. D. Chung, and Z. Wang, “Speaker-aware monaural speech separation,” in *Proc. INTERSPEECH*, 2020, pp. 1451–1455.
- [7] C. Knapp and G. Carter, “The generalized correlation method for estimation of time delay,” *IEEE Trans. Acoust., Speech, Signal Process.*, vol. 24, no. 4, pp. 320–327, 1976.
- [8] R. Schmidt, “Multiple emitter location and signal parameter estimation,” *IEEE Trans. Antennas Propag.*, vol. 34, no. 3, pp. 276–280, 1986.
- [9] J. DiBiase, H. Silverman, and M. Brandstein, “Robust localization in reverberant rooms,” in *Microphone Arrays: Signal Processing Techniques and Applications*, pp. 157–180. Springer, 2001.
- [10] W. He, P. Motlicek, and J. Odobez, “Deep neural networks for multiple speaker detection and localization,” in *Proc. IEEE Int. Conf. Robot. Autom.*, 2018, pp. 74–79.
- [11] D. Shmuel, J. Merkofer, G. Revach, R. Van Sloun, and N. Shlezinger, “Deep root MUSIC algorithm for data-driven DoA estimation,” in *Proc. IEEE Int. Conf. Acoust., Speech, Signal Process.*, 2023, pp. 1–5.
- [12] P. Pertilä and E. Cakir, “Robust direction estimation with convolutional neural networks based steered response power,” in *Proc. IEEE Int. Conf. Acoust., Speech, Signal Process.*, 2017, pp. 6125–6129.
- [13] L. Perotin, R. Serizel, E. Vincent, and A. Guérin, “CRNN-based multiple DoA estimation using acoustic intensity features for Ambisonics recordings,” *IEEE J. Sel. Topics Signal Process.*, vol. 13, no. 1, pp. 22–33, 2019.
- [14] S. Chakrabarty and E. Habets, “Multi-speaker DOA estimation using deep convolutional networks trained with noise signals,” *IEEE J. Sel. Topics Signal Process.*, vol. 13, no. 1, pp. 8–21, 2019.
- [15] X. Qian, M. Madhavi, Z. Pan, J. Wang, and H. Li, “Multi-target DoA estimation with an audio-visual fusion mechanism,” in *Proc. IEEE Int. Conf. Acoust., Speech, Signal Process.*, 2021, pp. 4280–4284.
- [16] Q. Li, X. Zhang, and H. Li, “Online direction of arrival estimation based on deep learning,” in *Proc. IEEE Int. Conf. Acoust., Speech, Signal Process.*, 2018, pp. 2616–2620.
- [17] S. Adavanne, A. Politis, J. Nikunen, and T. Virtanen, “Sound event localization and detection of overlapping sources using convolutional recurrent neural networks,” *IEEE J. Sel. Topics Signal Process.*, vol. 13, no. 1, pp. 34–48, 2018.
- [18] Z. Li and D. Hoiem, “Learning without forgetting,” *IEEE Trans. Pattern Anal. Mach. Intell.*, vol. 40, no. 12, pp. 2935–2947, 2017.
- [19] J. Schwarz, W. Czarnecki, J. Luketina, A. Grabska-Barwinska, Y. Teh, R. Pascanu, and R. Hadsell, “Progress & compress: A scalable framework for continual learning,” in *Proc. Int. Conf. Mach. Learn.* PMLR, 2018, pp. 4528–4537.
- [20] S. Rebuffi, A. Kolesnikov, G. Sperl, and C. Lampert, “iCaRL: Incremental classifier and representation learning,” *Proc. IEEE Conf. Comput. Vis. Pattern Recognit.*, pp. 5533–5542, 2017.
- [21] F. Cermelli, M. Mancini, S. Bulo, E. Ricci, and B. Caputo, “Modeling the background for incremental learning in semantic segmentation,” in *Proc. IEEE/CVF Conf. Comput. Vis. Pattern Recognit.*, 2020, pp. 9233–9242.
- [22] H. Zhuang, Z. Weng, R. He, Z. Lin, and Z. Zeng, “GKEAL: Gaussian kernel embedded analytic learning for few-shot class incremental task,” in *Proc. IEEE/CVF Conf. Comput. Vis. Pattern Recognit.*, 2023, pp. 7746–7755.
- [23] H. Zhuang, R. He, K. Tong, Z. Zeng, C. Chen, and Z. Lin, “DS-AL: A dual-stream analytic learning for exemplar-free class-incremental learning,” in *Proc. AAAI Conf. Artif. Intell.*, 2024.
- [24] H. Zhuang, Y. Chen, D. Fang, R. He, K. Tong, H. Wei, Z. Zeng, and C. Chen, “GACL: Exemplar-free generalized analytic continual learning,” *Adv. Neural Inf. Process. Syst.*, vol. 37, pp. 83024–83047, 2024.
- [25] H. Zhuang, Y. Liu, R. He, K. Tong, Z. Zeng, C. Chen, Y. Wang, and L. Chau, “F-OAL: Forward-only online analytic learning with fast training and low memory footprint in class incremental learning,” in *Adv. Neural Inf. Process. Syst.*, 2024, vol. 37, pp. 41517–41538.
- [26] X. Qian, X. Yue, J. Wang, H. Zhuang, and H. Li, “Analytic class incremental learning for sound source localization with privacy protection,” *IEEE Signal Process. Lett.*, vol. 32, pp. 726–730, 2025.
- [27] X. Liu, Y. Hu, X. Cao, A. Bagdanov, K. Li, and M. Cheng, “Long-tailed class incremental learning,” in *Proc. Eur. Conf. Comput. Vis.* Springer, 2022, pp. 495–512.
- [28] D. Fang, Y. Zhu, R. Fang, C. Chen, Z. Zeng, and H. Zhuang, “AIR: Analytic imbalance rectifier for continual learning,” *arXiv preprint arXiv:2408.10349*, 2024.
- [29] V. Raja et al., “Exploring challenges and solutions in cloud computing: A review of data security and privacy concerns,” *J. Artif. Intell. Gen. Sci.*, vol. 4, no. 1, pp. 121–144, 2024.
- [30] H. Zhuang, Z. Weng, H. Wei, R. Xie, K. Toh, and Z. Lin, “ACIL: Analytic class-incremental learning with absolute memorization and privacy protection,” *Adv. Neural Inf. Process. Syst.*, vol. 35, pp. 11602–11614, 2022.